

## Supporting Information

# Two-Dimensional Molecular Brush-Based Ultrahigh Edge-Nitrogen-Doped Carbon Nanosheets for Ultrafast Potassium-Ion Storage

Zongheng Cen, Youchen Tang, Junlong Huang, Yongqi Chen, Haozhen Yang,  
Dongtian Miao, Dingcai Wu \* and Shaohong Liu \*

PCFM Lab, School of Chemistry, Sun Yat-sen University,  
Guangzhou 510006, China

\* Correspondence: wudc@mail.sysu.edu.cn (D.W.);  
liushh27@mail.sysu.edu.cn (S.L.)

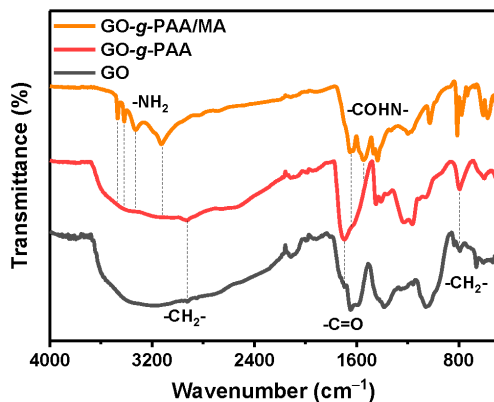


**Figure S1.** FT-IR spectra of GO, GO-g-PAA and GO-g-PAA/MA.

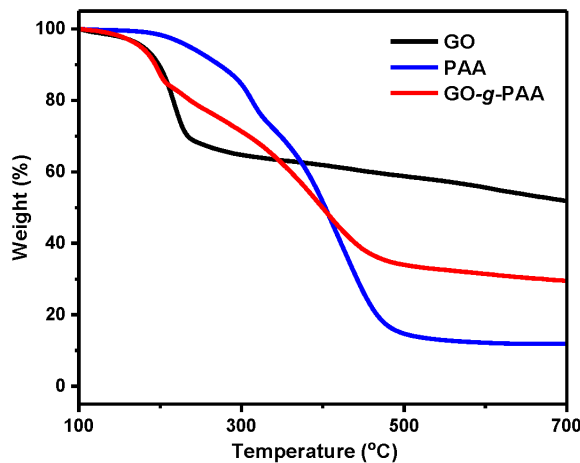


**Figure S2.** TGA curves of GO, PAA and GO-g-PAA.

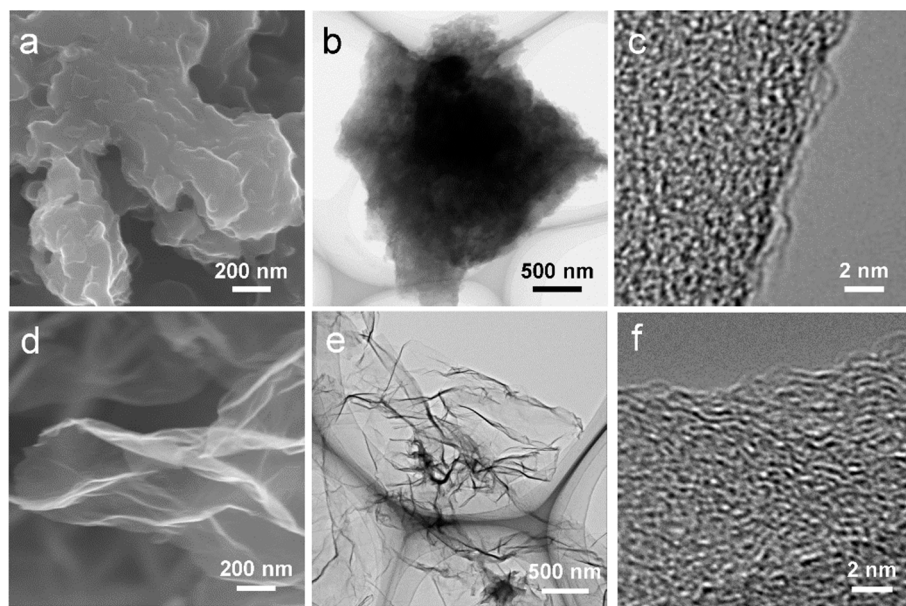


**Figure S3.** SEM, TEM and HRTEM images of (a-c) ENCNP and (d-f) CNS.

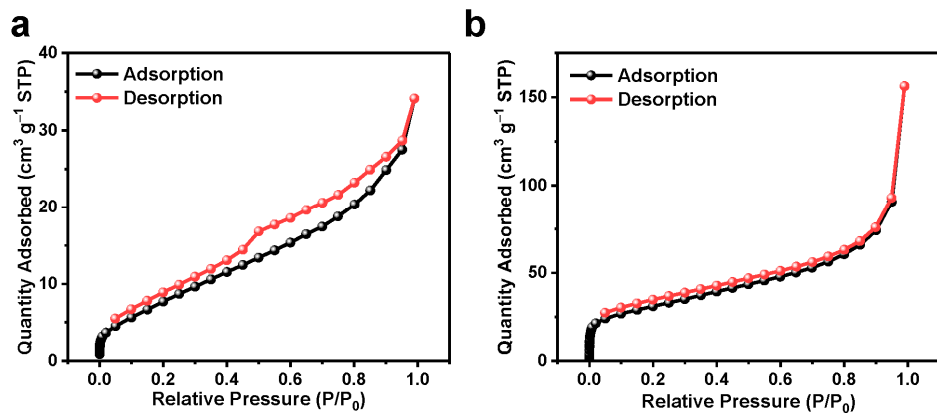


**Figure S4.**  $\text{N}_2$  adsorption-desorption isotherms of (a) ENCNP and (b) CNS.

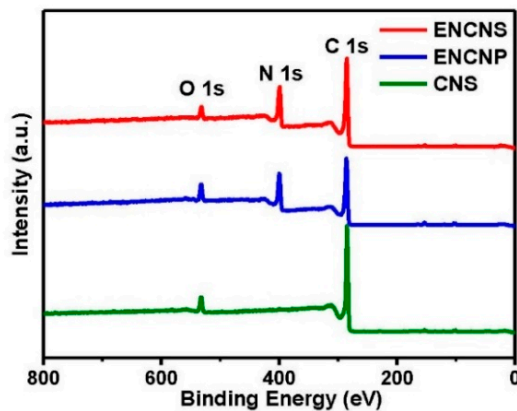


**Figure S5.** XPS full scans of ENCNS, ENCNP and CNS, revealing the presence of C, N and O elements.

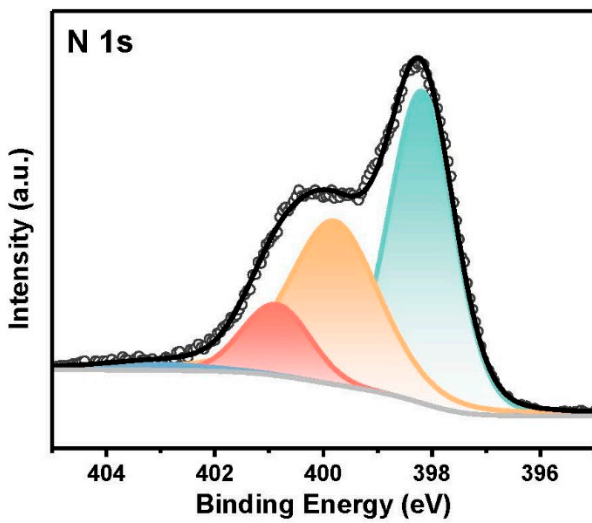


**Figure S6.** High-resolution N 1s XPS spectrum of ENCPN.

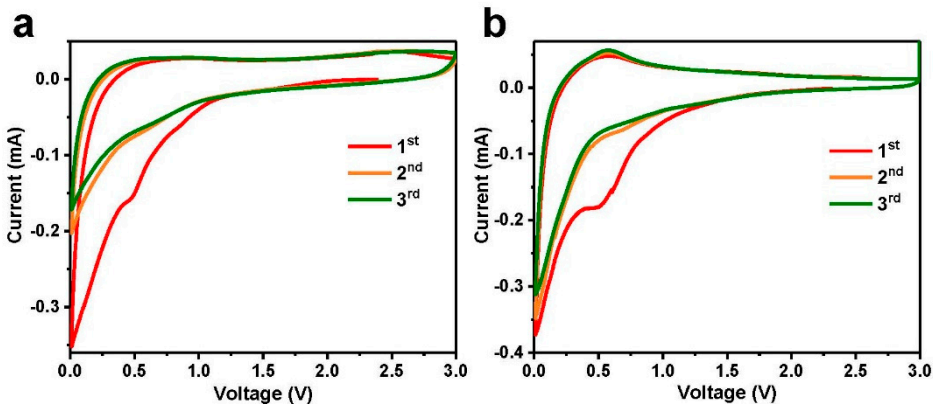


**Figure S7.** CV curves of (a) ENCPN and (b) CNS anodes at a scan rate of  $0.2 \text{ mV s}^{-1}$ .

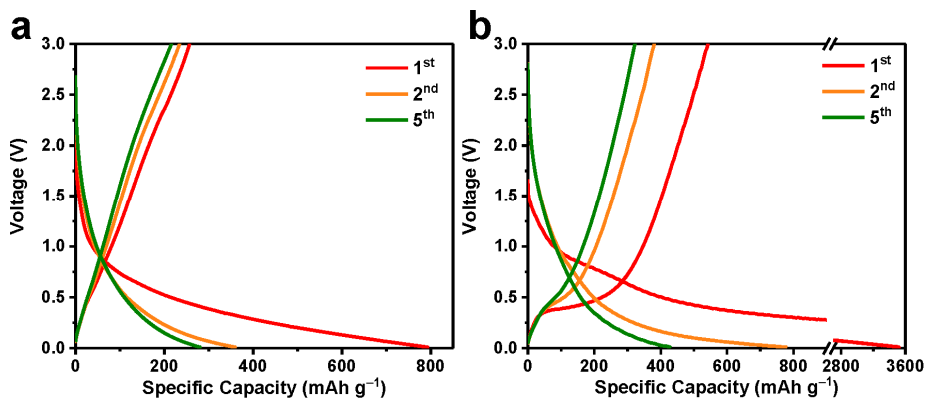


**Figure S8.** Discharge/charge curves of (a) ENCPN and (b) CNS anodes at a current density of  $0.05 \text{ A g}^{-1}$ .

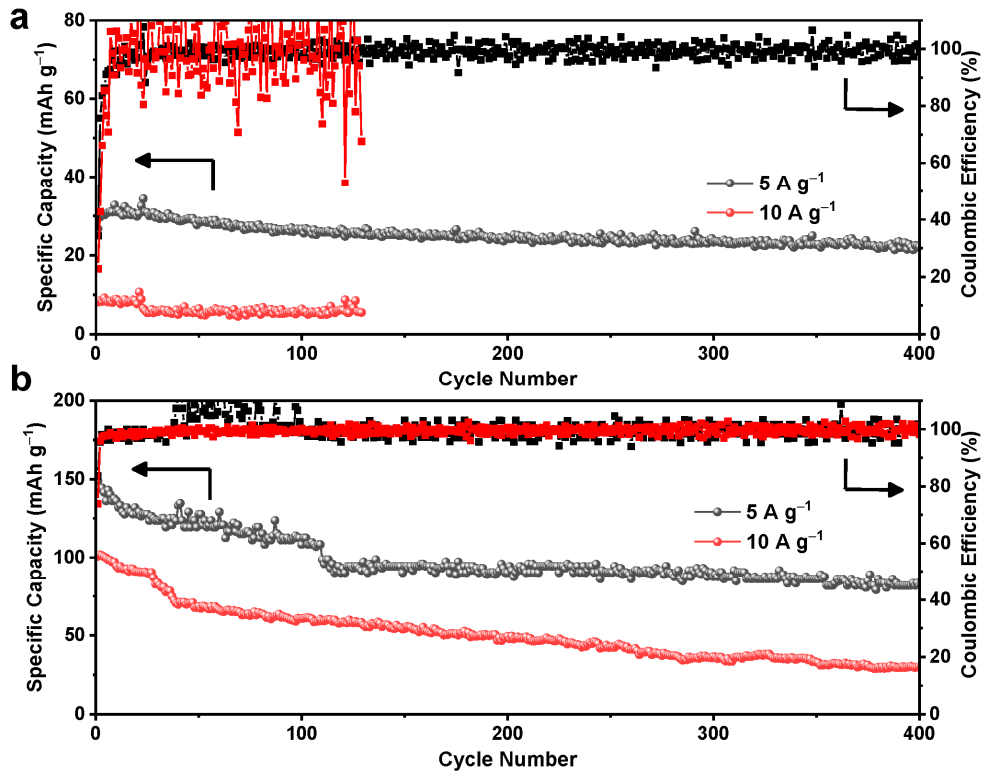


**Figure S9.** Long-term cycling performances of (a) ENCNP and (b) CNS at 5 and 10  $\text{A g}^{-1}$ .

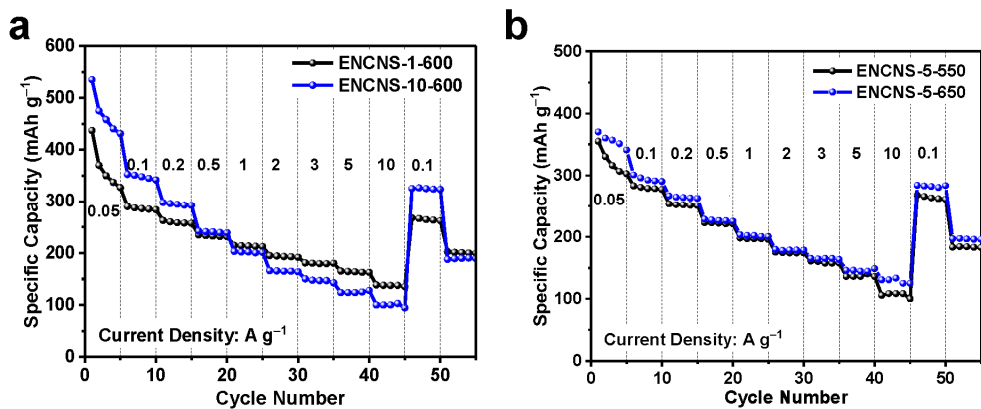


**Figure S10.** Rate capability of (a) ENCNS-1-600 and ENCNS-10-600 as well as (b) ENCNS-5-550 and ENCNS-5-650 at various current densities between 0.05 and 10.0  $\text{A g}^{-1}$ .

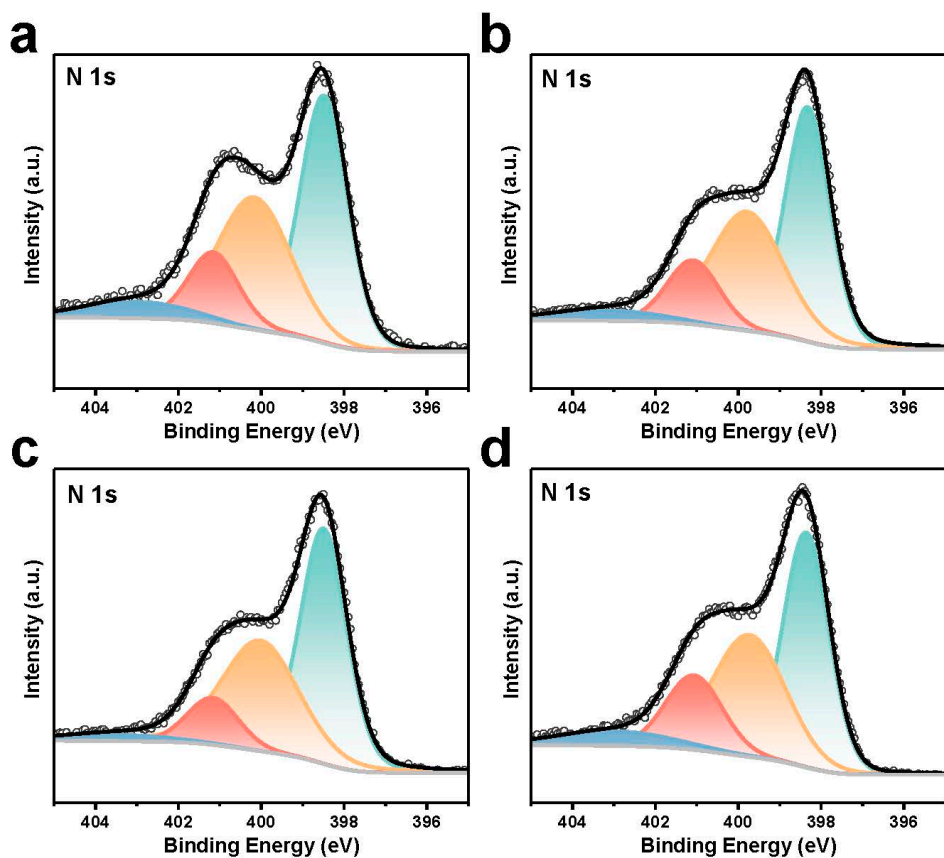


**Figure S11.** High-resolution N 1s XPS spectra of (a) ENCNS-1-600, (b) ENCNS-10-600, (c) ENCNS-5-550, and (d) ENCNS-5-650.

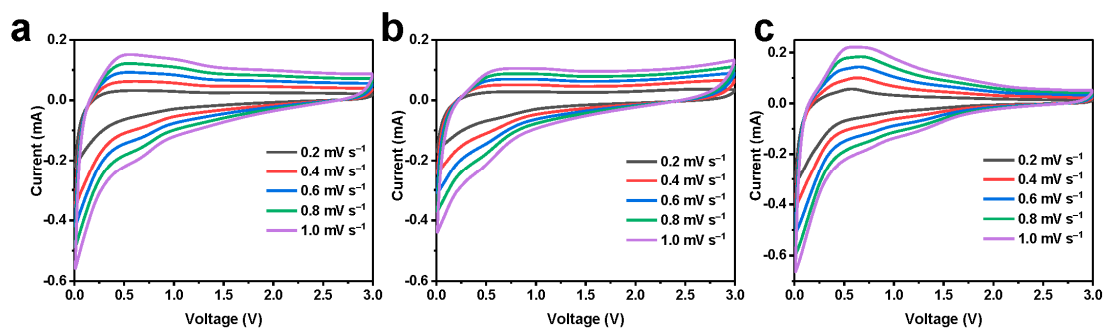


**Figure S12.** CV curves of (a) ENCNS, (b) ENCNP, and (c) CNS at scan rates of 0.2, 0.4, 0.6, 0.8 and  $1.0 \text{ mV s}^{-1}$ .

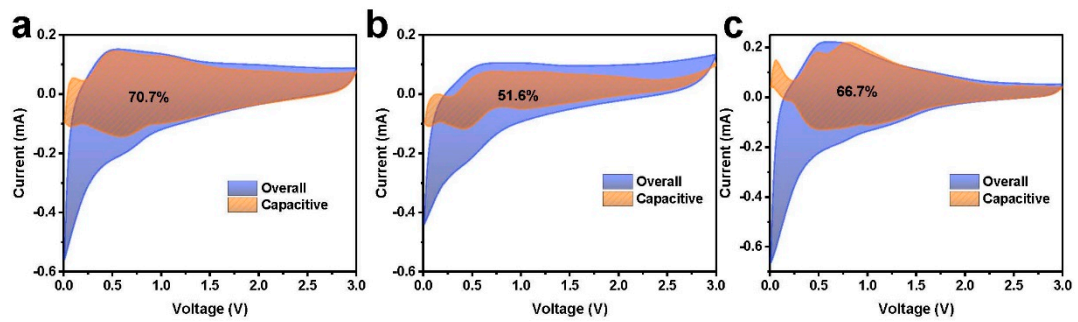


**Figure S13.** Capacitive contributions of (a) ENCNS, (b) ENCNP, and (c) CNS at a scan rate of 1.0  $\text{mV s}^{-1}$ .

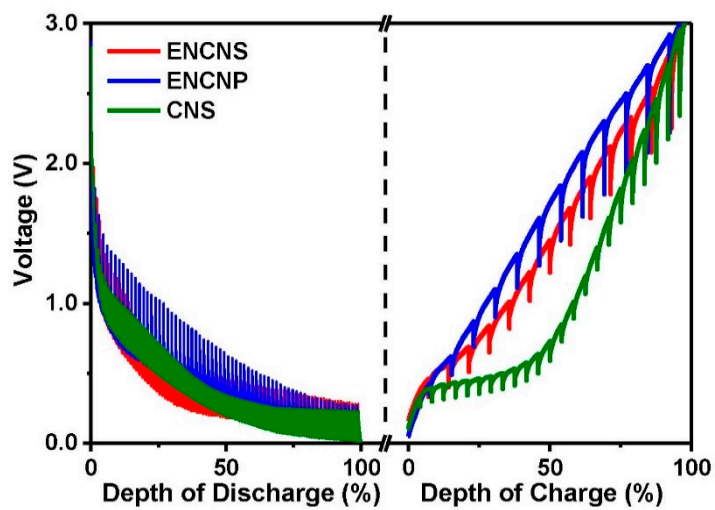


**Figure S14.** GITT potential profiles of ENCNS, ENCNP, and CNS.

**Table S1.** Total nitrogen and edge-nitrogen contents of various samples obtained with different molar ratios of -NH<sub>2</sub>/-COOH and heat treatment temperatures.

Sample	Total nitrogen content (at%)	N6 content (at%)	N5 content (at%)	NQ content (at%)	NO content (at%)	Edge- nitrogen content (at%)
<b>ENCNS</b>	20.6	8.5	7.7	2.8	1.6	16.2
<b>CNS</b>	0.6	-	-	-	-	-
<b>ENCNP</b>	22.4	10.9	8.7	2.4	0.4	19.6
<b>ENCNS-5-550</b>	24.1	11.6	9.3	2.5	0.7	20.9
<b>ENCNS-5-650</b>	19.3	8.1	6.7	3.2	1.3	14.8
<b>ENCNS-1-600</b>	9.3	4.1	3.4	1.3	0.5	7.5
<b>ENCNS-10-600</b>	21.6	9.4	8.3	3.0	0.9	17.7

**Table S2.** Total nitrogen content, edge-nitrogen content, and reversible capacity at  $5 \text{ A g}^{-1}$  of ENCNS and other reported nitrogen-doped carbonaceous anode materials in PIBs.

Sample	Total nitrogen content (at%)	Edge-nitrogen content (at%)	Reversible capacity at $5 \text{ A g}^{-1}$ (mAh g $^{-1}$ )	Reference
<b>ENCNS</b>	20.6	16.2	168	<b>This work</b>
<b>HNC</b>	17.03	15.70	93.0	[1]
<b>N-CNFs</b>	13.1	7.2	144	[2]
<b>NPPC-2-700</b>	3.68	2.82	133	[3]
<b>MCS-7-900</b>	5.27	1.96	107.9	[4]
<b>NCSN</b>	8.10	5.91	149	[5]
<b>ENDC</b>	10.5	9.2	74	[6]
<b>NSC</b>	2.09	1.57	115	[7]
<b>HENC</b>	5.78	4.38	101	[8]
<b>NCTP</b>	11.7	9.0	134.7	[9]
<b>HOCNs</b>	16.54	12.58	136	[10]
<b>N-PCNS</b>	12.1	11.8	127.5	[11]
<b>3DNFC</b>	5.74	5.02	115	[12]
<b>NCNFs</b>	13.8	7.7	126	[13]

## Reference

1. Huang, R.; Cao, Y. P.; Qin, S. Y.; Ren, Y. X.; Lan, R. C.; Zhang, L. Y.; Yu, Z.; Yang, H. Ultra-high N-doped open hollow carbon nano-cage with excellent Na<sup>+</sup> and K<sup>+</sup> storage performances. *Mater Today Nano*, **2022**, *18*, 100217.
2. Gong, J.; Zhao, G. Q.; Feng, J. K.; Wang, G. L.; Shi, Z. L.; An, Y. L.; Zhang, L.; Li, B. Control of the structure and composition of nitrogen-doped carbon nanofoams derived from CO<sub>2</sub> foamed polyacrylonitrile as anodes for high-performance potassium-ion batteries. *Electrochim Acta*, **2021**, *388*, 138630.
3. Ma, X. Q.; Xiao, N.; Xiao, J.; Song, X. D.; Guo, H. D.; Wang, Y. T.; Zhao, S. J.; Zhong, Y. P.; Qiu, J. S. Nitrogen and phosphorus dual-doped porous carbons for high-rate potassium ion batteries. *Carbon*, **2021**, *179*, 33-41.
4. Zheng, J. F.; Wu, Y. J.; Tong, Y.; Liu, X.; Sun, Y. J.; Li, H. Y.; Niu, L. High capacity and fast kinetics of potassium-ion batteries boosted by nitrogen-doped mesoporous carbon spheres. *Nano-Micro Lett*, **2021**, *13*, 174.
5. Bi, H. H.; He, X. J.; Yang, L.; Li, H. Q.; Jin, B. Y.; Qiu, J. S. Interconnected carbon nanocapsules with high N/S co-doping as stable and high-capacity potassium-ion battery anode. *J Energy Chem*, **2022**, *66*, 195-204.
6. Zhang, W. L.; Cao, Z.; Wang, W. X.; Alhajji, E.; Emwas, A.-H.; Costa, P. M. F. J.; Cavallo L.; Alshareef, H. N. A site-selective doping strategy of carbon anodes with remarkable K-ion storage capacity. *Angew Chem Int Ed*, **2020**, *59*, 4448-4455.
7. Liu, Q. D.; Han, F.; Zhou, J. F.; Li, Y.; Chen, L.; Zhang, F. Q.; Zhou, D. W.; Ye, C.; Yang, J. X.; Wu, X.; Liu, J. S. Boosting the potassium-ion storage performance in soft carbon anodes by the synergistic effect of optimized molten salt medium and N/S dual-doping. *ACS Appl Mater Inter*, **2020**, *12*, 20838-20848.
8. Zhao, Y.; Sun, Z. T.; Yi, Y. Y.; Lu, C.; Wang, M. L.; Xia, Z.; Lian, X. Y.; Liu, Z. F.; Sun, J. Y. Precise synthesis of N-doped graphitic carbon via chemical vapor deposition to unravel the dopant functions on potassium storage toward practical K-ion batteries. *Nano Res*, **2021**, *14*, 1413-1420.
9. Wang, K.; Li, N. N.; Sun, L.; Zhang, J.; Liu, X. H. Free-standing N-doped carbon nanotube films with tunable defects as a high capacity anode for potassium-ion batteries. *ACS Appl Mater Inter*, **2020**, *12*, 37506-37514.
10. Liu, S. T.; Yang, B. B.; Zhou, J. S.; Song, H. H. Nitrogen-rich carbon-onion-constructed nanosheets: An ultrafast and ultrastable dual anode material for sodium and potassium storage. *J Mater Chem A*, **2019**, *7*, 18499-18509.
11. Zhang, D. M.; Chen, Z. W.; Bai, J.; Yang, C. C.; Jiang, Q. Highly nitrogen-doped porous carbon nanosheets as high-performance anode for potassium-ion batteries. *Batteries Supercaps*, **2020**, *3*, 185-193.
12. Yang, B. J.; Chen, J. T.; Liu, L. Y.; Ma, P. J.; Liu, B.; Lang, J. W.; Tang, Y.; Yan, X. B. 3D nitrogen-doped framework carbon for high-performance potassium ion hybrid capacitor. *Energy Storage Mater*, **2019**, *23*, 522-529.
13. Xu, Y.; Zhang, C. L.; Zhou, M.; Fu, Q.; Zhao, C. X.; Wu, M. H.; Lei, Y. Highly nitrogen doped carbon nanofibers with superior rate capability and cyclability for potassium ion batteries. *Nat Commun*, **2018**, *9*, 1720.